2013 IEEE/RSJ International Conference on
Intelligent Robots and Systems (IROS)
November 3-7, 2013. Tokyo, Japan

Stabilizing Humanoids on Slopes Using Terrain Inclination Estimation

Zhibin Li, Nikos G. Tsagarakis, and Darwin G. Caldwell

Abstract— **This paper presents an integrated control framework for balancing humanoids on uneven terrains combining stabilization control and terrain inclination estimation. The stabilization is realized by passivity based admittance control that utilizes the force/torque feedback in feet to actively regulate the compliance. The logic-based terrain estimation algorithm exploits feet to probe the terrain inclination and deals with under-actuation when feet tilt on the contact surface. The equilibrium position in the admittance control is thereby adapted for recovering balance on the slope. Both the theoretical work and experimental validation are presented. The method is implemented and validated on the real humanoid by demonstrating the capability of estimating terrain inclination, balancing on the slope with varying gradient, and maintaining upright posture in the meantime. Experimental data such as inclination estimation in the comparison study, center of pressure measurement, and body attitude compensation are presented and analyzed.**

I. Introduction

To execute stable interaction in the environment with uncertainty, the passivity property is favored for robots in order to suppress undesired energy particularly delivered by the interaction forces. The passivity property is characterized by the negative rate change of system's energy, in other words, the system constantly attenuates energy, which is essential for manipulators with fixed bases [1] [2] and the humanoid robots that walk in human environment [3] [4].

The passivity property can be exploited for balancing humanoids such that the energy delivered by the disturbance decays so the system eventually returns to its equilibrium. This can be achieved by the impedance control approach using fully torque controlled systems such as the Sarcos humanoid [4], [5] or the DLR-biped [6], [7]. The common ground of these work is to compute the desired joint torque based on the Cartesian impedance defined at center of mass (COM) level for maintaining balance, and to distribute the contact forces through the support polygon by the joint torque control. Since most robots have position controlled actuators, we are motivated to investigate an admittance controller using the force/torque feedback in feet to modify the joint position references for achieving the passivity property. The viability of formulating the passivity based admittance control will be shown, and its performance will be further demonstrated by different experiments in this paper.

Some past work has proposed the compliance control to absorb landing impact and adapt terrain inclination for position controlled robots. The work in [8] proposed a PI control to superimpose an angular deviation of the ankle joint using the inclination measurement from torso. Strong low-pass filtering was applied for the inertial measurement unit (IMU) feedback, so the algorithm is suitable for a globally inclined surface rather than a slope with changing gradient. The WL-16R biped locomotor applied PD control with normalized gains to directly formulate the translational and angular acceleration of the waist, and used double integral to obtain the positional compensation since the robot has no force/torque control [9]. Their experiments demonstrated adaptation to a surface with a constant inclination of $8°$. However, the algorithm hasn't shown yet whether it could adapt to a rapidly changing slope. The predictive attitude control of WL-16RII [10] integrated the ZMP errors to compute the compensation for the pitch and roll angles. The integral control was only applied for a fixed time window and reset at each foot step to prevent windup. Our previous work in [11] also applied the similar integral control to compensate for the inclination upto $6.5°$. However, the integral control is good at removing steady-state errors but poor in dynamic response to varying gradient due to a low control bandwidth.

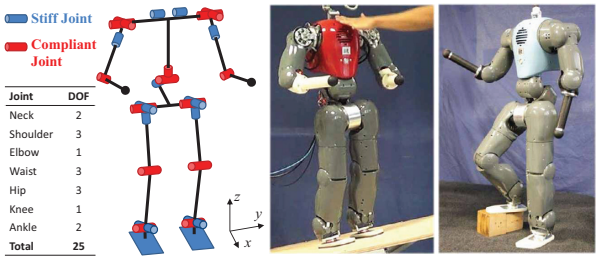

Fig. 1. COMAN humanoid and its kinematic and actuator configurations.

This paper contributes a control framework that permits the **CO**mpliant Hu**MAN**oid COMAN [12] to explore the terrain inclination through foot-ground contacts and adapt uneven surfaces by an admittance based compliance controller, as shown in Fig. 1. The terrain inclination estimation obtains the terrain surface information by contact exploration. Using the detected inclination, the equilibrium point in the admittance control is steered so as to accommodate the uneven surface.

The paper is organized as follows. Section II presents the compliance regulation using the passivity based admittance control and elaborates the principles of the terrain inclination estimation. Section III presents the experimental validation of the inclination estimation and stabilization on slopes with changing gradient. We conclude the study in Section IV.

This work is supported by the FP7 European projects AMARSi (ICT-248311) and WALK-MAN (ICT-2013-10).

Zhibin Li, Nikos G. Tsagarakis, and Darwin G. Caldwell are with the Department of Advanced Robotics, Istituto Italiano di Tecnologia, via Morego 30, 16163 Genova, Italy.
Email: zhibin.li@iit.it, nikos.tsagarakis@iit.it, darwin.caldwell@iit.it

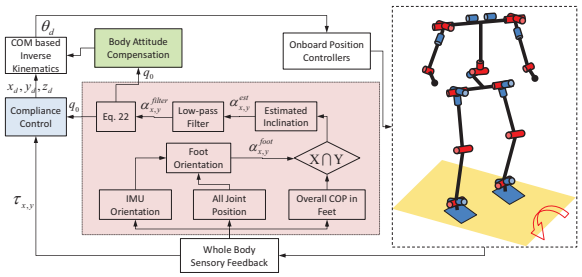

Fig. 2. Control framework for stabilization on cross slope.

II. Control Principles

The COMAN robot is a full body robot developed based on the compliant leg prototype in [13]. Fig. 1 shows the kinematics and the compliant joints allocations. The proposed control framework is illustrated in Fig. 2. The blue module is the compliance based stabilization control, the purple module is the terrain inclination detection that modulates the equilibrium in the stabilization control to adapt inclined surface, and the green module is the body attitude compensation for keeping the waist in an upright posture.

A. Compliance based Stabilization Control

The reference frame $\sum_B$ used in the following formulation is the local frame attached in the polygon formed by two feet. The origin of $\sum_B$ is the midpoint of the horizontal projections of two ankle joints. In the case of changing slope, $\sum_B$ moves together with the polygon while the world coordinate $\sum_W$ stays stationary. In $\sum_B$, the equivalent torsional stiffness K_s at the COM is contributed by both the gain k_p in motor PD control as well as the physical elasticity k_s from the compliant joints, so $K_s = \frac{k_p k_s}{k_p + k_s}$. Detailed identification of K_s can be found in [14]. The robot is simplified as a single rigid body mounted on the top of an inverted pendulum with mass m and moment of inertia I_c around the COM, as shown in Fig. 3(a).

The proposed admittance control uses the F/T sensor feedback from feet to compute the resultant torque generated by the ground reaction forces, and modulates the COM reference to produce the compliant behavior as that of a desired spring-damper system. In the admittance controller, the input is the resultant torque, the output of is the positional reference. As shown in Fig. 3(a), given the resultant stiffness K_s, the torque applied around the pivot can be regulated by controlling the reference COM position. Hence, in the real system, changing the COM reference modulates the real torque applied to the system, which follows the physical causality of "force→motion" for replicating the motion of a virtual system with passivity.

The parameters used in the admittance control are listed in Table I. The dynamics of this 1-DOF model in Fig. 3(a) is described by

$$I\ddot{q} = \tau_{ext} + \tau_g + K_s(\theta_d - q) + B(\dot{\theta}_d - \dot{q}). \quad (1)$$

The term τ_g is the gravitational torque

$$\tau_g = mglsin(q + \alpha), \quad (2)$$

TABLE I

Parameters used in admittance control

I:	inertia tensor around the pivot $I = I_c + mr^2$
m:	mass of the system
l:	nominal pendulum length from the COM to the pivot
θ_d:	desired angular position reference
θ_s:	angle of the spring deflexion
q:	real angular position of the pendulum
K_s:	resultant physical stiffness of the COM around pivot
B:	real viscous coefficient of the system around the pivot
K_d:	desired spring constant of the impedance
B_d:	desired viscous coefficient of the impedance

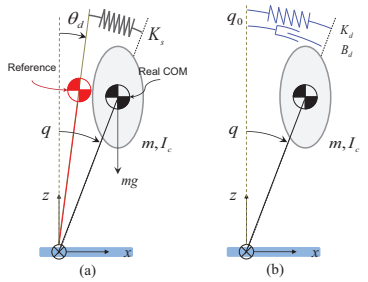

Fig. 3. Model for admittance control (sagittal view).

where α is the inclination of terrain surface.

The real damping B of the system is negligible, so the dynamics of the system can be approximated by

$$I\ddot{q} = \tau_{ext} + \tau_g + K_s(\theta_d - q), \quad (3)$$

which implies that the torque applied from the base to the pendulum is determined by the spring deflexion $K_s(\theta_d - q)$.

As shown in Fig. 3(b), the desired spring-damper system to be emulated has gravity compensation, a desired spring K_d ($K_d < K_s$) and a damper B_d connected between the equilibrium and the real COM. Only the stiffness and damping are the controlled properties and the inertia is kept the same. Hence, the dynamics of this desired system is

$$I\ddot{q} = \tau_{ext} + K_d(q_0 - q) + B_d(\dot{q}_0 - \dot{q}). \quad (4)$$

Therefore, if the net torque exerted by the gravity and spring deflexion is equal to the desired torque defined by the virtual spring damper system such as

$$\tau_g + K_s(\theta_d - q) = K_d(q_0 - q) + B_d(\dot{q}_0 - \dot{q}), \quad (5)$$

then these two systems would have the same dynamic response from the observation at the COM level.

Note that the term $K_s(\theta_d - q)$ implies the possibility of controlling the torque by θ_d to satisfy (5) via active regulation of the spring deflexion.

Rearrange (5), we obtain the relation between the reference position θ_d based on the real COM position.

$$\theta_d = \frac{K_d}{K_s}q_0 + \frac{K_s - K_d}{K_s}q + \frac{B_d}{K_s}(\dot{q}_0 - \dot{q}) - \frac{\tau_g}{K_s}, \quad (6)$$

The above is the method of modulating the reference to achieve a desired impedance based on the feedback of COM position and velocity. The control law can be reformulated

by the relation between torque and spring deflexion. Denote by τ the torque applied at the system in $\sum_B$, we have

$$\begin{cases} \tau &= -K_s\theta_s, \\ q &= \theta_d + \theta_s. \end{cases} \tag{7}$$

So q and $\dot{q}$ can be obtained as

$$\begin{cases} q &= \theta_d - \frac{\tau}{K_s}, \\ \dot{q} &= \dot{\theta}_d - \frac{\dot{\tau}}{K_s}. \end{cases} \tag{8}$$

Substitute (8) into (6), yields

$$\begin{aligned} \theta_d = \frac{K_d}{K_s}q_0 + \frac{B_d}{K_s}\dot{q}_0 + \frac{K_s - K_d}{K_s}\theta_d - \frac{B_d}{K_s}\dot{\theta}_d \\ - \frac{K_s - K_d}{K_s^2}\tau + \frac{B_d}{K_s^2}\dot{\tau} - \frac{\tau_g}{K_s}. \end{aligned} \tag{9}$$

The desired angular velocity $\dot{\theta}_d$ can be substituted by the derivative of the ideal reference using the backward Euler method

$$\dot{\theta}_d = \frac{\theta_d(i) - \theta_d(i-1)}{T}. \tag{10}$$

Substitute (10) into (9), we can derive the desired reference angle θ_d in the discrete form at the i th control loop, given feedback $\tau(i)$ and the control loop time T,

$$\theta_d(i) = \frac{T}{K_dT + B_d}A(i) + \frac{B_d}{K_dT + B_d}\theta_d(i-1), \tag{11}$$

where A is the intermediate variable

$$\begin{aligned} A(i) = K_dq_0(i) + B_d\dot{q}_0(i) + \frac{K_d - K_s}{K_s}\tau(i) \\ + \frac{B_d}{K_s}\dot{\tau}(i) - \tau_g(i). \end{aligned} \tag{12}$$

Setting $K_s \to \infty$ in (12) results in the admittance control formula for a stiff system without physical compliance where A evolves to

$$A(i) = K_dq_0(i) + B_d\dot{q}_0(i) - \tau(i) - \tau_g(i). \tag{13}$$

If the robot stands on the surface with inclination $\alpha(i)$, the gravity torque used in (12) and (13) is approximated by

$$\tau_g(i) = mglsin(\theta_d(i-1) - \frac{\tau(i)}{K_s} + \alpha(i)). \tag{14}$$

For a 1-DOF system, (11) is the general equation to achieve the admittance control. Equation (12) is used for the system with intrinsic elasticity, whereas (13) is for a system with ideal stiff coupling between gear transmission and link.

The above equations are derived in the rotational form, therefore, the following formulation follow the spherical coordinate to apply the proposed 1-DOF controller for the 3D robot. The subscripts/superscripts x, y in all the rotational variables indicate that the variable is defined about the x, y axis. The spatial motion of the COM is decomposed into the sagittal and lateral planes and controlled separately. The corresponding referential COM position in the Cartesian space can be converted as

$$\begin{cases} z_d &= l \cdot cos(atan2(\sqrt{(tan\theta_d^x)^2 + (tan\theta_d^y)^2}, 1)), \\ x_d &= z \cdot tan\theta_d^y, \\ y_d &= z \cdot tan(-\theta_d^x). \end{cases} \tag{15}$$

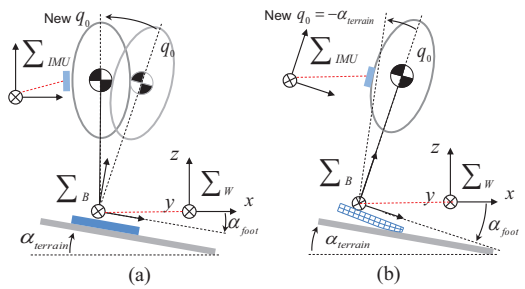

Fig. 4. Adapting inclined surface (a) ideal system, (b) real robot.

The desired COM position is the input of the COM based inverse kinematics and the details can be found in [14]. The outputs of the COM based inverse kinematics are the joint position references sending to on board position controllers. Note that the torque applied at joints are caused by the deformation of transmission elasticity, the position controllers have no direct torque control. The horizontal components of the resultant torque in $\sum_B$ are computed by

$$\boldsymbol{\tau}_{x,y} = \{\boldsymbol{\tau}_l + \boldsymbol{\tau}_r + \mathbf{r}_{f_l} \times \mathbf{f}_l + \mathbf{r}_{f_r} \times \mathbf{f}_r\}_{x,y}, \tag{16}$$

where τ_l, f_l and τ_r, f_r are the force/torque measured by the F/T sensor in each foot. r_{f_l} and r_{f_r} are the position vector from the origin of $\sum_B$ to the origin of F/T sensor in left and right foot respectively.

B. Exploring Terrain Inclination

Assume an ideal rigid robot whose feet are firmly placed at the terrain surface, the inclination of feet and terrain are identical, as shown in Fig. 4(a). On this assumption, to adapt the inclined surface becomes fairly straightforward by changing the equilibrium point in the admittance controller for keeping an upright posture. Though in reality, the robot is a floating base system whose feet can only provide unilateral force. Therefore, the foot could rotate around its edge in which case the inclinations of real surface and the foot are not always the same, as suggested in Fig. 4(b). Once the foot tilts, it forms an under-actuation phase that the torque around the foot edge is always zero. In this case, if the robot mistakes the foot inclination as the terrain inclination, it will change the equilibrium in such a way that the produced motion would make the foot tilt even more since the under-actuation DOF has no torque. The robot may ultimately lose balance by applying this wrong reaction.

To solve this instability issue in the under-actuation phase, we introduce the logic judgement for estimating terrain inclination that discretely activate or deactivate the updating process depending on the foot-ground contact. The feet are therefore used to probe the terrain information if no other means such as vision is utilized.

Fig. 5 shows different contact situations to illustrate the relation between the inclination of foot and terrain. The real foot has rubber pad that undergoes unavoidable deformation due to the load, so when the resultant ground reaction force acts near feet's edge, the foot is already slightly tilted, shown

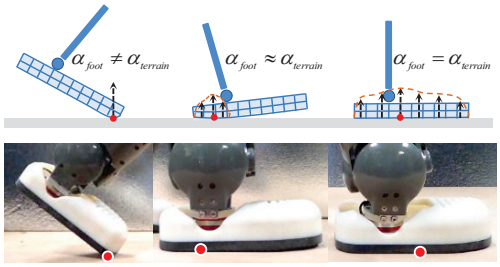

Fig. 5. Exploration of terrain inclination via foot-ground contact.

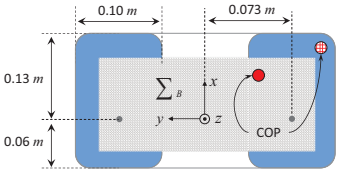

Fig. 6. Defining a firm contact region for logic-based inclination judgement.

by the central picture in Fig. 5. Therefore, the foot can only be a valid probe of the terrain inclination if it is loaded properly on the surface.

Similar to the body proprioception of humans, the orientation of the left/right foot are computed by combining both the IMU measurement and all the joint angles,

$$R_f^l = R_{IMU} R_{1\leftarrow 6}^l, \tag{17a}$$
$$R_f^r = R_{IMU} R_{1\leftarrow 6}^r, \tag{17b}$$

where R_{IMU} and $R_{1\leftarrow 6}^{l,r}$ are the orientation of the IMU with respect to the world, and the left/right foot with respect to the waist. The IMU is mounted on the waist of the robot.

Let $\mathbf{k}_l$ and $\mathbf{k}_r$ be the normal unit vectors in feet's local frames along z axis, the normal vector along z axis in $\sum_B$ with respect to the world frame is estimated as

$$\mathbf{k}_b = \frac{R_f^l \mathbf{k}_l + R_f^r \mathbf{k}_r}{||R_f^l \mathbf{k}_l + R_f^r \mathbf{k}_r||}. \tag{18}$$

The inclination $\boldsymbol{\alpha}^{foot}$ of the base frame $\sum_B$ is

$$\begin{cases} \alpha_x^{foot} = atan2(-k_b(y), k_b(z)), \\ \alpha_y^{foot} = atan2(k_b(x), k_b(z)). \end{cases} \tag{19}$$

To avoid a wrong estimation in the under-actuation phase, the estimation of terrain inclination $\boldsymbol{\alpha}^{est}$ only updates the sampled inclination $\boldsymbol{\alpha}^{foot}$ when the overall COP resides in a restricted region in the convex hull formed by two feet, shown by the grey area in Fig. 6.

$$\begin{cases} \boldsymbol{\alpha}^{est}(i) = \boldsymbol{\alpha}^{foot}(i), \text{iif } \mathbf{X} \cap \mathbf{Y}, \\ \boldsymbol{\alpha}^{est}(i) = \boldsymbol{\alpha}^{foot}(i-1), \text{otherwise}, \end{cases} \tag{20}$$

where

$$\begin{cases} \mathbf{X} &= \left\{ x : x_{cop}^{min} < x_{cop}^{-} \leq x_{cop} \leq x_{cop}^{+} < x_{cop}^{max} \right\}, \\ \mathbf{Y} &= \left\{ y : y_{cop}^{min} < y_{cop}^{-} \leq y_{cop} \leq y_{cop}^{+} < y_{cop}^{max} \right\}. \end{cases} \tag{21}$$

The boundary limits are identified experimentally by constantly pushing the robot till the feet start tilting. The values are $x_{cop}^{-} = -0.03m$, $x_{cop}^{+} = 0.10m$, $y_{cop}^{-} = -0.095m$, $y_{cop}^{+} = 0.095m$. The maximum values of x_{cop} and y_{cop} are defined by the polygon's dimension (Fig. 6), $x_{cop}^{max} = 0.13m$, $x_{cop}^{min} = -0.06m$, $y_{cop}^{max} = 0.123m$, $y_{cop}^{min} = -0.123m$.

When the COP is detected outside the grey area as shown in Fig. 6, the rubber in feet deforms under the pressure so the inclination of foot is not identical to that of the terrain. Therefore, the proposed logic condition $\mathbf{X} \cap \mathbf{Y}$ implies a firm foot placement on the terrain such that $\boldsymbol{\alpha}^{est} = \boldsymbol{\alpha}^{foot}$ is the most probable. The estimation $\boldsymbol{\alpha}^{est}$ holds its previous value if $\mathbf{X} \cap \mathbf{Y}$ is not satisfied. For example, when feet rotate on the slope, we have $\boldsymbol{\alpha}^{est} \neq \boldsymbol{\alpha}^{foot}$, so the foot inclination $\boldsymbol{\alpha}$ should not be assigned to the estimation of terrain inclination $\boldsymbol{\alpha}^{est}$. In a variety of experimental investigations, we found $\boldsymbol{\alpha}^{est}$ very useful to prevent wrong estimation of terrain inclination particularly when feet significantly tilt.

In turn, the logical judgment introduces discrete values into $\boldsymbol{\alpha}^{est}$, therefore its filtered data $\boldsymbol{\alpha}^{filter}$ are used to update the equilibrium point $\mathbf{q}_0$ as in (22). With the above algorithms, the whole robot will behave as a passive spring-damper system with a fixed equilibrium when feet tilt, and actively dissipate excessive energy until the feet conform to terrain surface again assuming that the push is not large enough to completely topple the robot.

In order to adapt the inclined slope, the equilibrium point of the replicated spring-damper system is updated with respect to the base frame $\sum_B$

$$\boldsymbol{q}_0 = -\boldsymbol{\alpha}^{filter}, \tag{22}$$

in accordance with the terrain inclination as illustrated in Fig. 4(b). $\boldsymbol{q}_0$ contains the inclination in the sagittal and lateral planes, and is substituted into (12) to update the equilibrium.

The unit vector $\mathbf{r}$ of the updated equilibrium point is

$$\begin{cases} r_z &= cos(atan2(\sqrt{(tanq_0^x)^2 + (tanq_0^y)^2}, 1)), \\ r_x &= r_z \cdot tanq_0^y, \\ r_y &= r_z \cdot tan(-q_0^x). \end{cases} \tag{23}$$

In the base frame $\sum_B$, the orientation of the upper body is compensated as

$$R_{body} = R_{rodrigues}(\boldsymbol{\omega}_n, \varphi), \tag{24}$$

where the intermediate variables are

$$\begin{cases} \varphi = atan2(\sqrt{r_x^2 + r_y^2}, r_z), \\ \mathbf{v} = [r_x, r_y, 0]^T, \\ \mathbf{v}_n = \mathbf{v}/||\mathbf{v}||, \\ \boldsymbol{\omega}_n = R_z(90^\circ)\mathbf{v}_n, \end{cases} \tag{25}$$

in order to keep the waist in an upright posture. $R_{rodrigues}$ is Rodrigues' rotation formula, and $\boldsymbol{\omega}_n$ is the unit vector around which the angular rotation φ is performed.

III. Experiments

To examine the proposed control framework, three experiments were designed to validate the effectiveness. Real experiments can be viewed in the accompanied video.

The parameters used for the experiments are as follows. The cutoff frequency of the low-pass filters is $8Hz$ for

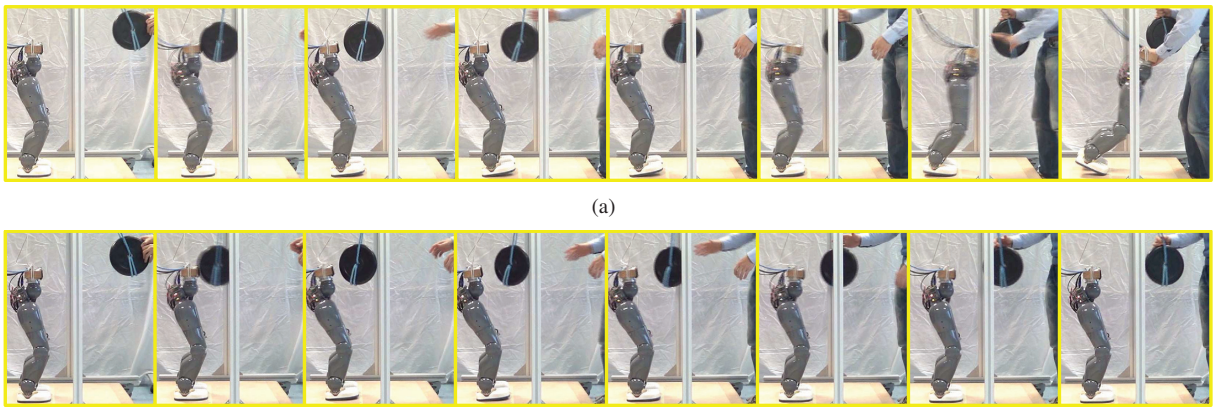

(a)

(b)

Fig. 7. Experiment I: stabilization against impact without (a) and with (b) logic based terrain estimation (time spaced 1/6s since 2nd snapshot).

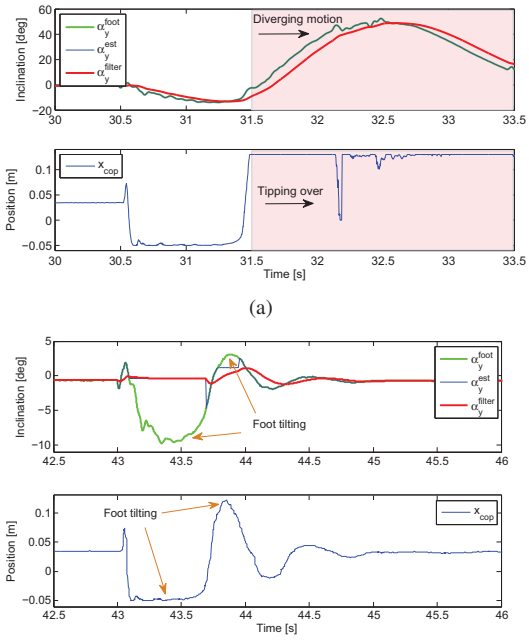

(a)

(b)

Fig. 8. Experiment I: estimation of foot/ground inclination and the COP response without (a) and with (b) logic-based terrain estimation.

filtering $\boldsymbol{\alpha}_{x,y}^{est}$. The desired stiffness and viscous coefficient are $K_d^y = 110Nm/rad$, $B_d^y = 50Nms/rad$ around the y axis (sagittal plane), and $K_d^x = 225Nm/rad$, $B_d^x = 135Nms/rad$ around the x axis (lateral plane).

A. Experiment I

In this comparison study, a $5kg$ weight was suspended with a pendulum length of $0.75m$. The initial angle of the pendulum was $25°$, the angle at the instant of impact was $5°$, so the speed of weight right before imapct was $1.15m/s$. The impact was the same for both tests.

Fig. 7(a) shows the snapshots of impact test without the logic-based terrain estimation, the assumption $\boldsymbol{\alpha}^{est} = \boldsymbol{\alpha}^{foot}$ always holds so that the robot was mistaken the foot inclination as the terrain inclination when under-actuation

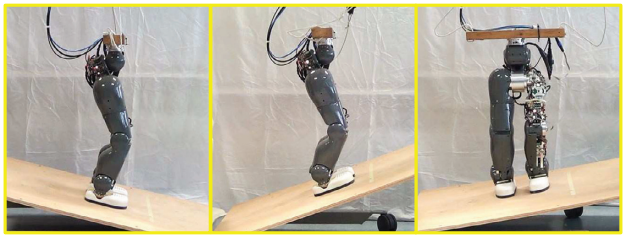

Fig. 9. Experiment II: adapting inclined terrain in the sagittal and lateral planes respectively.

phase occurs as shown in Fig. 8(a), whereas the ground is flat. In this case, the robot tilted up feet to adapt a fictitious surface as if it stood on an inclined terrain. This can been seen in the 5th snapshot in Fig. 7(a), and the COP measurement from $30.5s$ to $31.5s$ in Fig. 8(a). Therefore, the robot ultimately overthrew itself while returning to the central position after $31.5s$ shown by the diverging motion in Fig. 7(a) and Fig. 8(a).

On the other hand, with the logic-based terrain estimation, the robot held the most recent and reliable estimation of terrain inclination when the feet were rotating around their edges as shown in Fig. 8(b) during $43 - 44s$. In this case, the equilibrium point in the stabilization control was kept the same so that the whole system behaved the same as a passive system defined by the desired stiffness K_d and damping B_d, dissipating the excessive energy delivered by the impact. As shown by the snapshots in Fig. 7(b) and experimental data in Fig. 8(b), it prevented the over tilting problem of feet and the robot recovered its posture after impact.

B. Experiment II

The 2nd experiment demonstrates the stabilization capability on the slope with large inclination variation shown by the snapshots in Fig. 9. In order to validate the performance on changing slope given the fixed parameters of the controller, a time-varying inclination was applied with peak-to-peak amplitude of $14°$ and period of $2.8s$. This inclination was chosen to apply around the negative direction of y axis, meaning that the disturbance leaned the robot backward,

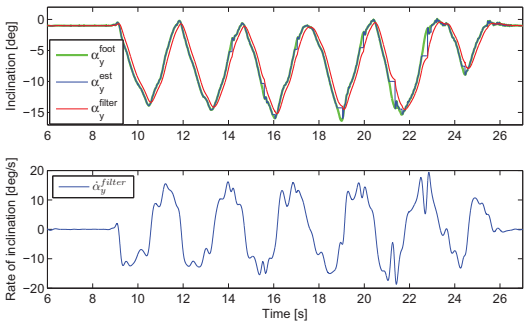

Fig. 10. Experiment II: estimation of terrain inclination on rapid changing slope.

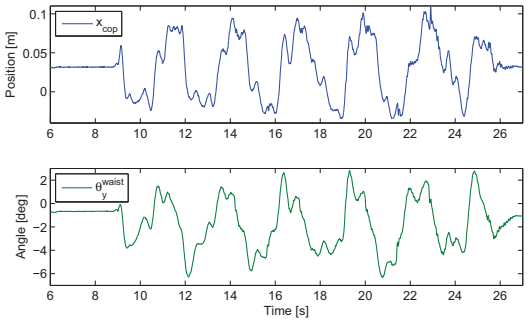

Fig. 11. Experiment II: COP and body attitude variations during the rapid change of terrain inclination.

which was the most challenging scenario for balancing in standing posture.

Fig. 10 shows the estimated terrain inclination α_y^{filter} and its rate $\dot{\alpha}_y^{filter}$. The average rate given by $\dot{\alpha}_y^{filter}$ data is $9.5°/s$. Fig. 11 shows that the variation of x_{cop} is within $(-0.04, 0.11)m$, and the pitch angle of waist is within $(-7, 3)°$.

C. Experiment III

The 3rd experiment is a balancing task on an emulated surfboard by combining the sagittal and lateral gradient variations. Fig. 12 shows the COMAN robot with a bottle of red liquid placed on the waist. During the disturbance, the control algorithms adapted the inclined board and kept the waist as level as possible, so the bottle stood stably.

IV. Conclusion

A control framework consists of a compliance based stabilizer and the terrain inclination estimation is proposed for stabilizing humanoids on changing slopes. The compliance control not only stabilizes the robot against impacts, but also improves feet's conformance with the ground. A logic-based terrain estimation algorithm exploits the foot-ground contact as a means to detect the terrain inclination. The integration of these modules are proved to be effective even during under-actuation phase when feet tilt. Different experiments in Section III show that COMAN could adapt slopes with changing inclination in both sagittal and lateral planes with a stabilized body attitude.

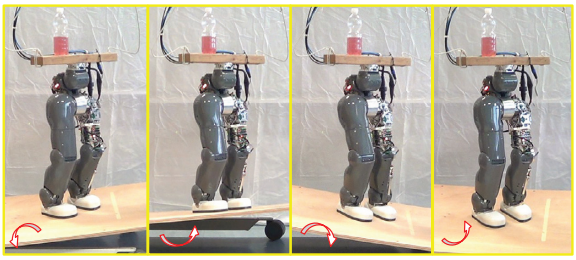

Fig. 12. Experiment III: balancing on slope with varying gradients in both sagittal and lateral planes.

References

[1] C. Ott, A. Albu-Schaffer, A. Kugi, S. Stamigioli, and G. Hirzinger, "A passivity based cartesian impedance controller for flexible joint robots-part i: Torque feedback and gravity compensation," in *IEEE International Conference on Robotics and Automation*, vol. 3, 2004, pp. 2659–2665.

[2] A. Albu-Schaffer, C. Ott, and G. Hirzinger, "A passivity based cartesian impedance controller for flexible joint robots-part ii: Full state feedback, impedance design and experiments," in *IEEE International Conference on Robotics and Automation*, vol. 3, 2004, pp. 2666–2672.

[3] S. Hyon and G. Cheng, "Passivity-based full-body force control for humanoids and application to dynamic balancing and locomotion," in *IEEE/RSJ International Conference on Intelligent Robots and Systems*, 2006, pp. 4915–4922.

[4] S. Hyon, J. Hale, and G. Cheng, "Full-body compliant human-humanoid interaction: Balancing in the presence of unknown external forces," *IEEE Transactions on Robotics*, vol. 23, no. 5, pp. 884–898, October 2007.

[5] B. Stephens and C. Atkeson, "Dynamic balance force control for compliant humanoid robots," in *IEEE/RSJ International Conference on Intelligent Robots and Systems*, 2010, pp. 1248–1255.

[6] C. Ott, C. Baumgartner, J. Mayr, M. Fuchs, R. Burger, D. Lee, O. Eiberger, A. Albu-Schaffer, M. Grebenstein, and G. Hirzinger, "Development of a biped robot with torque controlled joints," in *10th IEEE-RAS International Conference on Humanoid Robots*, 2010, pp. 167–173.

[7] C. Ott, M. Roa, and G. Hirzinger, "Posture and balance control for biped robots based on contact force optimization," in *11th IEEE-RAS International Conference on Humanoid Robots*, Bled, Slovenia, 2011, pp. 26–33.

[8] J. Kim, I. Park, and J. Oh, "Walking control algorithm of biped humanoid robot on uneven and inclined floor," *Journal of Intelligent & Robotic Systems*, vol. 48, no. 4, pp. 457–484, 2007.

[9] Y. Sugahara, Y. Mikuriya, K. Hashimoto, T. Hosobata, H. Sunazuka, M. Kawase, H. Lim, and A. Takanishi, "Walking control method of biped locomotors on inclined plane," in *IEEE International Conference on Robotics and Automation*, 2005, pp. 1977–1982.

[10] K. Hashimoto, Y. Sugahara, M. Kawase, A. Ohta, C. Tanaka, A. Hayashi, N. Endo, T. Sawato, H. Lim, and A. Takanashi, "Landing pattern modification method with predictive attitude and compliance control to deal with uneven terrain," in *IEEE/RSJ International Conference on Intelligent Robots and Systems*, 2006, pp. 1755–1760.

[11] Z. Li, B. Vanderborght, N. G. Tsagarakis, L. Colasanto, and D. G. Caldwell, "Stabilization for the Compliant Humanoid Robot COMAN Exploiting Intrinsic and Controlled Compliance," in *IEEE International Conference on Robotics and Automation*, 2012, pp. 2000–2006.

[12] N. Tsagarakis, S. Morfey, G. Medrano-Cerda, Z. Li, and D. Caldwell, "Compliant humanoid coman: Optimal joint stiffness tuning for modal frequency control," in *IEEE International Conference on Robotics and Automation (ICRA)*, 2013, pp. 665–670.

[13] N. Tsagarakis, Z. Li, J. A. Saglia, and D. G. Caldwell, "The design of the lower body of the compliant humanoid robot 'cCub'," in *IEEE International Conference on Robotics and Automation*, Shanghai, China, 2011, pp. 2035–2040.

[14] Z. Li, N. Tsagarakis, and D. G. Caldwell, "A passivity based admittance control for stabilizing the compliant humanoid COMAN," in *IEEE-RAS International Conference on Humanoid Robots*, Osaka, Japan, Nov. 29th - Dec. 1st 2012, pp. 44–49.